Photochemistry and Photobiology, 2006, 82: 31–37

Psoralen and Coumarin Photochemistry in HSA Complexes and DMPC Vesicles†

L. Chen, O. Rinco, J. Popov, N. Vuong and Linda J. Johnston*

Steacie Institute for Molecular Sciences, National Research Council Canada, Ottawa, ON, Canada

Received 20 July 2005; accepted 07 September 2005; published online 08 September 2005 DOI: 10.1562/2005-07-20-RA-616

ABSTRACT

The photochemistry and photophysics of several psoralens and coumarins have been examined in human serum albumin (HSA) complexes and dimyristoylphosphatidylcholine (DMPC) vesicles. Fluorescence spectroscopy indicates that there are multiple binding sites with polarities that are intermediate between those of acetonitrile and water for the substrates complexed to HSA. In the case of the 6,7-dimethoxycoumarin-HSA complex, laser flash photolysis experiments provide evidence for the formation of radical cation in addition to triplet. Radical cations are not detected for other coumarin-HSA complexes, either due to a lower yield of formation or to rapid reaction of an initial radical cation with adjacent amino acids. Fluorescence spectra for coumarins indicate that they are primarily solubilized in the polar headgroup region in DMPC vesicles. Consistent with this, radical cations generated by photoionization are detected in transient experiments. For dimethoxycoumarins the radical cation is long-lived, indicating rapid exit from the vesicle and decay in the aqueous phase. However, 4,5′,8-trimethylpsoralen and 7-ethoxy-4-hexadecylcoumarin radical cations are much shorter-lived, presumably due to rapid decay by electron recombination in the vesicle. The results for both HSA complexes and vesicles indicate that radical ions may play a role in psoralen and coumarin photochemistry in a cellular environment.

INTRODUCTION

The photochemistry and photophysics of psoralens and coumarins have been studied extensively because of their utility as photoactivated drugs (1–3). Psoralens in particular have seen widespread use in psoralen plus ultraviolet A (PUVA) therapy for treatment of dermatological conditions and virus inactivation (2,4). The mechanism for the therapeutic effects of PUVA therapy was initially believed to involve intercalation of psoralen between adjacent base pairs within the DNA duplex followed by two successive photochemical cycloaddition reactions that linked the coumarin and furan moieties to bases within the adjacent DNA strands. The resulting cross-link is responsible for inhibition of replication and cell proliferation. Despite the therapeutic effects of psoralens, there is increasing evidence relating their long-term use to harmful side effects such as carcinogenicity, mutagenicity, and immune system modulation (5,6). It is also clear that reactions other than DNA cross-linking are important in both the beneficial and deleterious effects of PUVA therapy. Photoaddition to membrane components, singlet oxygen-mediated chemistry, and reaction with amino acids and proteins have all been postulated, on the basis of a variety of studies both in model systems and in a cellular environment (7–15).

We have studied the direct photoionization of several psoralens and coumarins in aqueous environment and in micelles (16–18). The results demonstrate that monophotonic ionization occurs with significant quantum yield for appropriately substituted substrates (*e.g.* 0.2 for 6,7-dimethoxycoumarin [6,7-DMC]) in aqueous solution and that the yields are sensitive to the local environment. As an example, electrostatic effects favor higher photoionization yields in anionic sodium dodecyl sulfate (SDS) micelles, as compared to neutral or cationic micelles. The reactivity of psoralen and coumarin radical cations with DNA bases, amino acids and membrane components was also evaluated and was shown to be dominated by electron transfer reactions with readily oxidized substrates (18,19). Taken together our results indicate that electron transfer chemistry initiated by direct photoionization of psoralens may contribute to the *in vivo* chemistry of these photosensitizers.

We have now examined the photochemistry of representative psoralens and coumarins (Scheme 1) as complexes with human serum albumin (HSA) and in vesicles as more realistic models for cellular systems. Albumin has a high binding capacity for a wide range of endogenous and exogeneous ligands, making it a key determinant of the pharmokinetic behavior of many drugs (20) and a widely studied model protein. The choice of vesicles as membrane models is relevant since membrane localization and damage play an important role in various forms of photodynamic therapy (21,22). We were particularly interested in probing the possibility of photoionization and electron transfer-initiated chemistry in these environments. Understanding the photochemistry of coumarins in the presence of proteins and lipids is also relevant to the use of coumarin-labeled nucleotides as caged compounds for photorelease of adenosine triphosphate and

* To whom correspondence should be addressed: Address. Steacie Institute for Molecular Sciences, National Research Council Canada, Ottawa, ON K1A 0R6, Canada. Fax: 613-952-0068; e-mail: Linda.Johnston@nrc-cnrc.gc.ca

† This paper is part of a special issue dedicated to Professor J. C. (Tito) Scaiano on the occasion of his 60th birthday.

Abbreviations: 7-AMC, 7-amino-4-methylcoumarin; 5,7-DMC, 5,7-dimethoxycoumarin; 6,7-DMC, 6,7-dimethoxycoumarin; DMPC, dimyristoylphosphatidylcholine; 7-EHC, 7-ethoxy-4-hexadecylcoumarin; 7-HOC, 7-hydroxycoumarin; HSA, human serum albumin; LFP, laser flash photolysis; 7-MOC, 7-methoxycoumarin; 8-MOP, 8-methoxypsoralen; PUVA, psoralen plus ultraviolet A; SDS, sodium dodecyl sulfate; TMP, 4,5′,8-trimethylpsoralen.

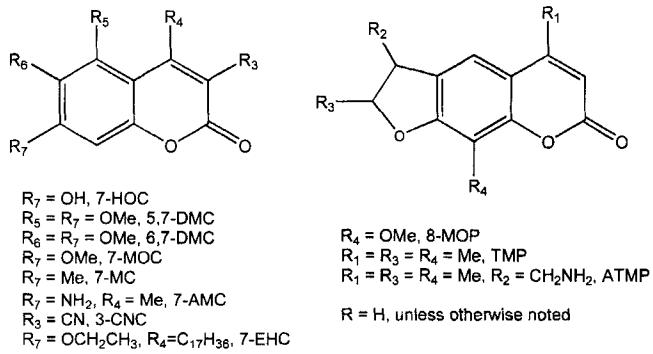

Scheme 1.

γ-aminobutyric acid for cellular studies (23,24). The results obtained in this study provide further support for our earlier findings concerning the importance of radical ions in psoralen and coumarin photochemistry.

MATERIALS AND METHODS

Chemicals. 3-Cyanocoumarin and 7-ethoxy-4-heptadecylcoumarin (7-EHC) were purchased from Indofine Chemicals (Hillsborough, NJ) and Molecular Probes (Eugene, OR), respectively. All other coumarins were from Aldrich (Oakville, ON, Canada) and were used as received. Fatty acid-free HSA (Sigma, Oakville, ON, Canada) and 1,2-dimyristoyl-*sn*-glycero-3-phosphocholine (DMPC; Avanti Polar Lipids, Alabaster, AL) were also used as received. All aqueous solutions were prepared in pH 7.4 phosphate buffer and all solvents were of the highest available commercial grade.

Sample preparation. For preparation of vesicles, the appropriate amounts of probe and phospholipids were dissolved in chloroform and then the chloroform was evaporated under a stream of nitrogen to deposit a lipid film on the sample vial. The sample was dried under vacuum overnight and then hydrated with pH 7.4 phosphate buffer to give a final lipid concentration of 1 mg/mL. Samples were sonicated with a microtip sonicator until clear and then filtered (0.22 μm) to eliminate large vesicles or debris from the sonicator tip.

HSA samples were prepared by dissolving HSA in an aqueous buffer solution of coumarin at the appropriate concentration for either fluorescence or laser flash photolysis (LFP) experiments. Solutions were mixed for 1 h at 37°C before use. Unless otherwise noted HSA concentration was between 0.3 and 0.5 mM for all experiments.

Fluorescence spectroscopy. Steady-state and time-resolved fluorescence data were recorded using a Photon Technology International (London, ON, Canada) fluorescence spectrometer equipped for single photon counting. Samples were contained in 10×10 mm^2 quartz cuvettes and were prepared with absorbance <0.1 at the excitation wavelength. Samples were purged with nitrogen for 30 min before use to remove oxygen. Decay traces were deconvoluted and fitted to either a single exponential or the sum of two exponentials using PTI software. Estimates of free and bound 6,7-DMC for variable concentrations of HSA were estimated from the decreases in fluorescence intensity as a function of complexation:

$$X = (I_p - I_{inf})/(I_0 - I_{inf})$$

where X is the fraction of bound DMC, I_p is the fluorescence intensity at a particular HSA concentration, and I_0 and I_{inf} are fluorescence intensities in the absence of HSA and at a HSA concentration where all DMC is bound (25). Fluorescence spectra were corrected for a weak residual emission from HSA alone.

LFP. The nanosecond laser system has been described in detail elsewhere (26). The excitation laser was a Lumonics HY750 Nd:YAG laser (Northville, MI; 355 nm, 10 ns/40 mJ pulses). Samples had a ground state absorbance between 0.2 and 0.5 at the excitation wavelength, were contained in 7×7 mm^2 quartz cells, and were degassed with nitrogen before use, unless otherwise noted.

Table 1. Fluorescence emission maxima for psoralens and coumarins in pH 7.4 aqueous buffer, acetonitrile, HSA complexes and DMPC vesicles

	λ_{em} (nm, buffer)	λ_{em} (nm, acetonitrile)	λ_{em} (nm, HSA)	λ_{em} (nm, DMPC)
7-Methylcoumarin	375	360	372	—
7-Methoxycoumarin	393	378	393	390
3-Cyanocoumarin	417	406	423	—
7-Ethoxy-4-hexadecylcoumarin	—	373	—	376
6,7-Dimethoxycoumarin	431	420	427	434
7-Amino-4-methylcoumarin	441	372	439	—
5,7-Dimethoxyocumarin	448	403	445	—
7-Hydroxycoumarin	455	381	388/425*	—
8-Methoxypsoralen	510†	—	501	—
4,5′,8-Trimethylpsoralen	471	422	438	461‡
4′-Aminomethyl-4,5′, 8-trimethylpsoralen	458	—	433	—

* Emission maxima of 390 and 425 nm were obtained for 328 and 370 nm excitation, respectively.
† Reference 28.
‡ Shoulder at 423 nm.

RESULTS AND DISCUSSION

HSA complexes

Fluorescence spectroscopy. Fluorescence spectra for a variety of psoralens and coumarins complexed to HSA were measured and the data are summarized in Table 1 and Figure 1, along with fluorescence data in acetonitrile and aqueous buffer. These data provide information on the polarity of the substrate binding site since several of the coumarins and psoralens show quite pronounced blue shifts in emission with decreasing solvent polarity (16,27,28). The fluorescence maxima for most of the HSA complexes were similar to or slightly blue-shifted from the λ_{max} values for the coumarin in water and were much closer to values in water than in acetonitrile. For example, 6,7-DMC has fluorescence maxima of 431, 420 and 386 nm in water, acetonitrile and decane, respectively. The measured λ_{max} of 427 nm for the HSA complex is consistent with a relatively polar binding site and is similar to values observed for micellar solution (423, 425 and 429 nm for SDS, cetyl trimethylammonium bromide and Triton-X 100 solutions) (16). Data for 5,7-dimethoxycoumarin (5,7-DMC) (Fig. 1) also show reasonably large shifts with solvent polarity and comparison of the fluorescence maxima of the HSA complex with those for homogeneous solution leads to similar conclusions. Psoralen-HSA complexes show larger blue shifts than do the coumarin complexes, consistent with the larger effects of solvent polarity for psoralens in homogeneous solution. As an example, 4,5′, 8-trimethylpsoralen (TMP) has fluorescence maxima at 368 nm in decane, 422 nm in acetonitrile, 468 nm in aqueous solution and 439 nm in SDS micellar solution (16). The observed fluorescence maximum of 438 nm for the HSA complex (Fig. 1g) thus indicates a protein binding site that is considerably more polar than acetonitrile and comparable to that of the micellar interface region. As shown in Fig. 1 for 5,7-DMC and TMP, the fluorescence spectra for HSA complexes are slightly broader than those obtained in either water or acetonitrile.

The shifts in fluorescence maximum for 7-hydroxycoumarin (7-HOC) have a different origin from the polarity-induced solvent shifts observed for the other substrates. 7-HOC has a pK_a value of

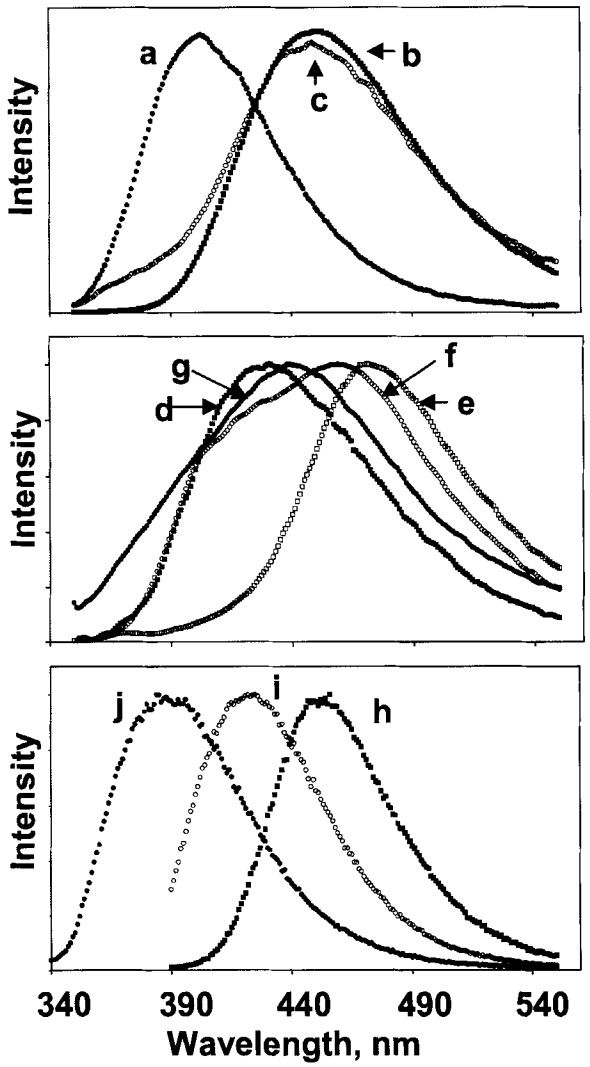

Figure 1. Normalized (on the basis of maximum intensity) fluorescence spectra for representative coumarins and psoralens: top, 5,7-DMC in acetonitrile (a), aqueous buffer (b), HSA complex in aqueous buffer (c); middle, TMP in acetonitrile (d), buffer (e), HSA complex (g) and DMPC vesicles (f); bottom, 7-HOC in aqueous buffer (h, 370 nm excitation), and 7-HOC-HSA complex in aqueous buffer with 328 nm (i) and 370 nm (j) excitation.

7.8 and the acidic and basic forms show distinct absorption maxima at 326 and 365 nm, respectively (29). Although fluorescence from protonated 7-HOC is readily detected in organic solvents (λ_{max} 370–380 nm), the fluorescence spectrum in aqueous solution shows λ_{max} at 452 nm over a range of pH values (from 5 to 12, Fig. 1h). This is due to rapid excited-state deprotonation to generate excited anion, with an excited-state pK_a value of 0.45 (29). The fluorescence of a number of 4-alkyl-7-hydroxycoumarins and related fluorophores has been used to probe the interfacial potential for micelles and vesicles (29–32). In the presence of HSA, the ground-state absorption of 7-HOC shows a maximum at ~365 nm, with little absorption at the maximum for the protonated form, indicating an aqueous (and basic) environment. Consistent with this, excitation at 370 nm gives an emission at 425 nm that is slightly shifted from the anion emission in aqueous buffer. However, 328 nm excitation gives a different emission spectrum with λ_{max} at 388 nm, indicative of a small amount of protonated 7-HOC, presumably in a much less aqueous environment (compare spectra i and j in Fig. 1). This suggests that there are two distinct binding sites for 7-HOC in HSA. Similarly, the broader spectra obtained for other HSA complexes as compared to pure solvents may reflect some heterogeneity of binding sites.

Table 2. Fluorescence lifetimes for coumarins in acetonitrile, pH 7.4 aqueous buffer and HSA complexes. Decay traces for all HSA complexes were fit to a sum of two exponentials

Coumarin	τ (AcN)	τ (buffer)	τ (HSA)
5,7-Dimethoxycoumarin	1.54 ± 0.03	7.23 ± 0.03	0.81 ± 0.08 (0.58) 4.30 ± 0.10 (0.42)
6,7-Dimethoxycoumarin	1.14 ± 0.01	4.30 ± 0.01	1.91 ± 0.06 (0.61) 5.07 ± 0.08 (0.39)
7-Methoxycoumarin	*	7.21 ± 0.05	1.29 ± 0.02 (0.7) 4.09 ± 0.04 (0.3)
7-Methylcoumarin	*	*	—
7-Amino-4-methylcoumarin	3.77 ± 0.07	4.75 ± 0.02	1.24 ± 0.06 (0.48) 5.18 ± 0.03 (0.52)
7-Hydroxycoumarin†	*	5.26 ± 0.02	2.40 ± 0.20 (0.72) 3.80 ± 0.30 (0.28)

* Not determined due to weak fluorescence.
† Excitation at 328 (buffer) and 370 (HSA) nm, emission at 425 nm.

Fluorescence lifetimes were measured for selected substrates in acetonitrile, aqueous buffer and HSA complexes and the data are listed in Table 2. The fluorescence decays for all coumarins give good fits to single exponential kinetics in both aqueous buffer and acetonitrile, with shorter lifetimes and substantially weaker signals observed for acetonitrile. By contrast, more complex decay kinetics were observed in all cases for the coumarin-HSA complexes. The decays gave very poor fits to a single exponential but were adequately fit by a sum of two exponentials (Table 2). In each case, there is a fast component that decays within 1–2 ns and a slower component with a lifetime of 4–5 ns. Although the relative amounts of the two vary there is always a substantial fraction (>~30%) of each. The shorter component for the decay is similar to the lifetimes in acetonitrile, whereas the slower component is similar to or slightly less than the value for the same compound in aqueous solution. These results are consistent with multiple binding sites, one of which shows intermediate polarity between acetonitrile and water and a second that is similar in polarity to acetonitrile. The fact that the fluorescence lifetimes for the complex are similar to or longer than those for the same substrates in acetonitrile suggests that the change in lifetime is related to the polarity of the binding site, rather than to direct quenching of the excited substrate by amino acids in the binding site. This is also supported by the similarity in trends for fluorescence emission maxima and lifetimes as a function of solvent polarity.

Several literature studies have examined the binding of warfarin (3-(α-acetonylbenzyl)-4-hydroxycoumarin) and related coumarins to HSA using equilibrium dialysis to assess the amounts of bound and free probe as a function of HSA concentration (33,34). Scatchard plots of the ratio of the concentrations of bound to free ligand *vs* the concentration of bound ligand showed pronounced curvature, indicative of multiple binding sites. Analysis of the binding curves was found to be consistent with two classes of binding sites, each with between one and three bound molecules. Dissociation constants (K_d) in the 1–100 μM range were determined, with coumarins with polar substituents showing stronger

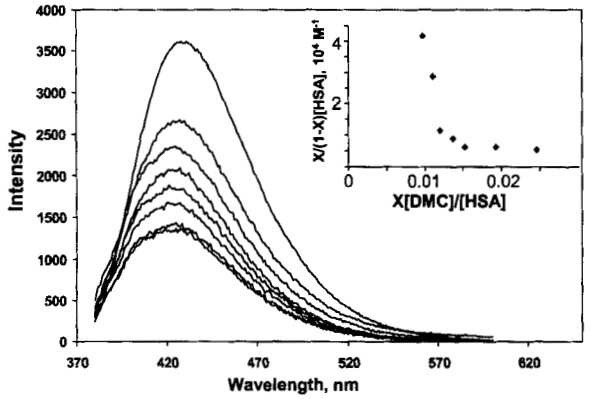

Figure 2. Changes in fluorescence intensity for 6,7-DMC as a function of HSA concentration; inset shows a Scatchard analysis based on calculating the fractions of free and bound probe from the fluorescence intensity data.

binding. For example, warfarin and 4-hydroxycoumarin had binding constants that were approximately one and two orders of magnitude larger than the unsubstituted coumarins. HSA consists of three structurally similar subdomains, each comprised of two subdomains (35). There is consensus in the literature that warfarin binds primarily to a site on subdomain IIA, which has a single tryptophan residue, although additional binding sites in domains I and III have also been suggested (33,34,36).

The fluorescence intensity for the various psoralens and coumarins decreased upon addition of HSA to an aqueous buffer solution, as shown in Fig. 2 for 6,7-DMC. This change in fluorescence intensity can be used to estimate the fraction of free and bound probes, provided that a constant limiting intensity is obtained at a high concentration of HSA. The 6,7-DMC fluorescence intensities at variable HAS concentrations were used to calculate fractions of bound *vs* free coumarin as outlined in the Materials and Methods section above and to generate a Scatchard plot as shown in Fig. 2 (25). The nonlinearity of the plot is indicative of multiple binding sites and is similar to the results obtained for several substituted coumarins (33,34). Although the relatively limited amount of data are not adequate for fitting to multiple sites as

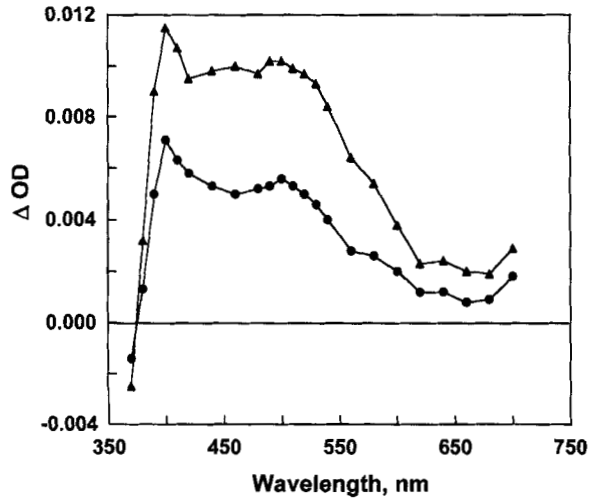

Figure 3. Transient absorption spectra obtained after 355 nm excitation of 6,7-DMC in 1.1 mM HSA: nitrogen (▲) with a delay of 160 ns and in oxygen (●) with a delay of 300 ns.

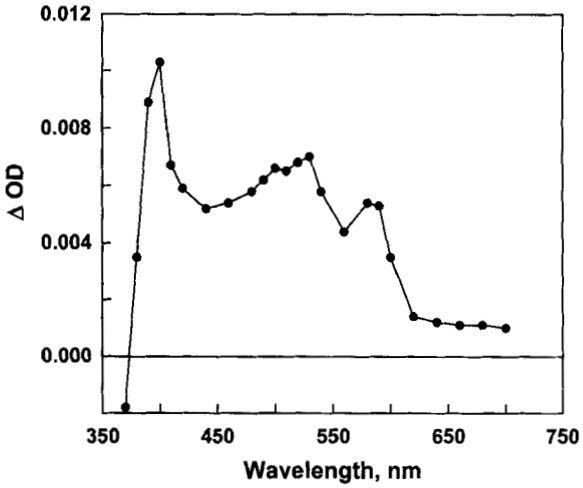

Figure 4. Transient absorption spectrum measured 320 ns after 355 nm excitation of 6,7-DMC in 0.5 mM HSA in the presence of oxygen.

in previous work, as described by Dahlquist (37), the initial linear range can be used to estimate that strong binding sites have a K_d value in the micromolar range, similar to previous determinations.

LFP. Transient absorption measurements were used to assess whether excitation of the coumarin- or psoralen-HSA complexes resulted in any net photochemistry. Previous LFP studies have shown that laser excitation of a variety of psoralens or coumarins in aqueous solution yields a mixture of triplet and radical cations (16–18). In several cases the photoionization is quite efficient; for example, 6,7-DMC has a quantum yield of 0.2 for radical cation production in aqueous solution (18). To ensure that aqueous photochemistry did not contribute significantly to our observed results, the LFP experiments for the HSA complexes were carried out at relatively high HSA/substrate ratios so as to minimize the amount of uncomplexed substrate.

Typical results obtained upon 355 nm laser excitation of 6,7-DMC/HSA in aqueous buffer are shown in Fig. 3. Oxygen-saturated solutions give a transient at 500 nm that decays over a timescale of 5 μs, in addition to a weaker signal in the 400 nm region that is produced in control experiments by direct excitation of HSA alone. Nitrogen-saturated solutions give a much broader absorption (Fig. 3). In neither case is there any evidence for a significant yield of radical cation that has λ_{max} at 590 nm (18). The decrease of the 500 nm signal in oxygen-saturated solutions is consistent with triplet formation, as is the fact that a number of methoxycoumarin triplets have absorptions in the 500 nm region. The residual 500 nm signal in the presence of oxygen may be due to a triplet that is well protected within its protein binding site and thus not accessible to oxygen. This is in agreement with the fact that the fluorescence lifetime data indicate at least two distinct binding sites of different polarity.

By contrast to the results above, experiments at lower HSA concentrations (0.5 mM, Fig. 4 *vs* 1.1 mM for Fig. 3) do show a small yield of radical cation with characteristic maxima at 390 and 590 nm. On the basis of the rough estimate for the association constant (see above), the amount of uncomplexed coumarin is <2% for both HSA concentrations, making it very unlikely that excitation of 6,7-DMC in the aqueous phase is responsible for the radical cation that we observe. The lack of detectable radical cation at higher HSA concentrations may reflect redistribution of the probe to a less polar site that does not lead to radical cation formation.

An alternative possibility is that the coumarin is photoionized even at high HSA concentrations but the initial radical cation is rapidly trapped by an adjacent amino acid. This may occur in the type IIA binding site, which has a single tryptophan residue. In fact the generation of a tryptophan-derived radical by deprotonation of an initial radical cation could also be responsible for some of the 500 nm signal that we observe. This hypothesis is consistent with the known spectrum for the tryptophan radical, with an absorption maximum at ~520 nm (38) and with our previous observation of rapid electron transfer to coumarin radical cations from tryptophan (19). Although solvated electrons are not detected at long wavelength in the transient studies for the HSA complex, photoejected electrons are likely to be rapidly scavenged by protein, precluding detection on our timescale.

Initial transient studies used 6,7-DMC because it is the most efficiently photoionized of the psoralens and coumarins that we had studied in our previous work. We also examined the transients obtained by excitation of complexes of 5,7-DMC and 4′-amino-4,5′,8-trimethylpsoralen with HSA. In both cases, we observed a similar transient at 500 nm for oxygen-saturated solution and a stronger broader signal in the 500 nm region for a nitrogen-purged solution, but no evidence for radical cation. The residual 500 nm signal in the presence of oxygen could be due either to triplet in a site that is not accessible to oxygen or to a tryptophan-derived radical generated by trapping of an initial coumarin or psoralen radical cation, as discussed above for 6,7-DMC. Note that we have no evidence for a route involving direct reaction of the excited probe with tryprophan, although we cannot absolutely exclude this possibility. By contrast to these results, laser excitation of 8-methoxypsoralen (8-MOP) did not give a 500 nm signal. The 8-MOP triplet absorbs at shorter wavelength (<400 nm) and the photoionization efficiency for 8-MOP is considerably lower than that for the methoxycoumarins. Either of these factors could be responsible for the lack of a 500 nm transient.

Vesicles

Fluorescence spectra and transient behavior were examined for four different psoralens and coumarins in DMPC vesicles. Fluorescence maxima for 7-EHC, 7-methylcoumarin and 6,7-DMC were 376, 390 and 434 nm, all of which are very similar to the values obtained in aqueous solution (see Table 1 and discussion above) and can be interpreted in terms of localization of the probe in the polar headgroup region of the vesicle. TMP showed more complex behavior with a fluorescence spectrum that was considerably broader than that in homogeneous solution and that was sensitive to the length of time and method of sonication used for sample preparation (Fig. 1). Relatively short sonication times showed more long wavelength emission (at 460 nm *vs* 471 nm in water), whereas longer sonication led to blue shifts in the fluorescence maximum, to a value of ~420 nm, indicating a less polar probe environment. The results are consistent with more than one solubilization site for TMP; although the relative contributions of the short and long wavelength emission varied with the sample preparation conditions, both were always present.

Transient absorption spectroscopy was used to evaluate the photoionization efficiency for representative psoralens and coumarins in DMPC vesicle solution. The results obtained by 355 nm excitation of 6,7-DMC in DMPC vesicles are shown in Fig. 5. Spectra for an oxygen-saturated sample showed signals at 590 and 390 nm, with bleaching of the starting material at 360 nm, in good

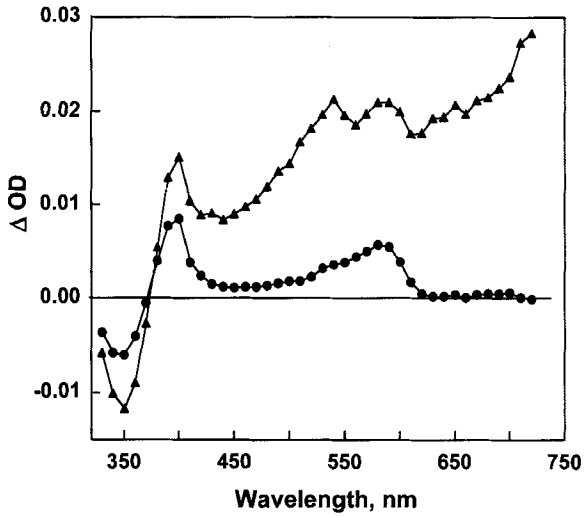

Figure 5. Transient absorption spectra measured after 355 nm excitation of 6,7-DMC in DMPC vesicles in the presence of nitrogen (▲, 1.4 μs) and oxygen (●, 1.6 μs).

agreement with published spectra for the DMC radical cation (18). The radical cation decays with a rate constant of *ca* 2×10^5 s^{-1} in vesicle solution as compared to 1×10^5 s^{-1} in aqueous solution. The spectrum under nitrogen shows broad absorptions between 400 and 700 nm, consistent with additional oxygen-sensitive signals due to both triplet (500 nm) and solvated electron (>600 nm). A similar experiment with 7-methoxycoumarin (7-MOC) also generated radical cation cleanly (λ_{max} at 630 nm) and with a decay rate constant of 0.6×10^5 s^{-1} as compared to 3×10^5 s^{-1} in aqueous solution. In this case, quenching of the radical cation with guanosine monophosphate (GMP) and tryptophan was also examined. Both resulted in efficient reaction with rate constants of 2.4×10^9 and 2.8×10^9 M^{-1} s^{-1} that are similar to those obtained for reaction of the radical cation in aqueous solution (4.1 and 4.2×10^9 M^{-1} $s^{-1}$for GMP and tryptophan, respectively) (19). Both the 7-MOC and 6,7-DMC radical cations decayed more rapidly when the lipid/probe ratio was decreased by a factor of 2 (from 50:1 to 25:1).

The efficiency of radical cation generation was similar in aqueous buffer and vesicles, on the basis of the observation that the 6,7-DMC radical cation yield for samples with matched absorbance at the laser wavelength was approximately 20% higher for aqueous solution than for DMPC vesicles. The slightly lower yield is consistent with the less polar environment experienced by the probe in the polar headgroup region of the vesicle.

The behavior of the more hydrophobic TMP in DMPC vesicles was also examined by LFP. The results show photoionization to give radical cation with λ_{max} at 640 nm, although the signals were weaker than those observed for the two coumarins. In this case the kinetics for decay of radical cation showed a short and a long component, which decayed with rate constants of 5×10^6 s^{-1} and 2×10^5 s^{-1}, respectively. The long-lived component is similar to the decay of the radical cation in 20% acetonitrile/water, $\sim 1 \times 10^5$ s^{-1} (16).

The similarity of the decay kinetics for the long-lived DMC and TMP radical cations in the presence and absence of quenchers to those in aqueous buffer suggests that the ions are in the aqueous phase, rather than in the vesicles. Since the fluorescence results are consistent with localization of the initial psoralens and coumarins

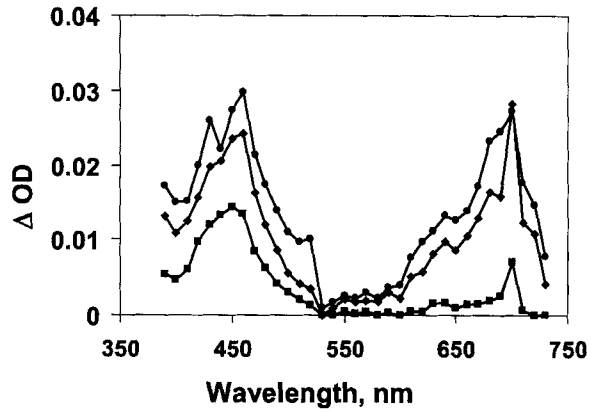

Figure 6. Transient absorption spectrum of the 7-EHC radical cation generated by 355 nm excitation of chloranil in acetonitrile in the presence of 1×10^{-3} M 7-EHC. Spectra were recorded 0.3, 1 and 4 μs after laser excitation.

in the vesicle interface region, this hypothesis requires relatively rapid exit of the radical cation from the vesicle. Although we cannot exclude a small amount of photoionization for residual aqueous-solubilized substrate for the two coumarins, this is unlikely to be the case for TMP, which is too insoluble in water for spectroscopic studies. Our previous work showed that the decay of the radical cations in buffer in the absence of quenchers was primarily limited by slow reaction with the precursor psoralen or coumarins. Thus, variation in the amount of residual substrate in the aqueous phase and accessibility of the micelle- or vesicle-localized substrate could account for the fact that our measured radical cation lifetimes are not identical to those in aqueous buffer. The variation in bimolecular quenching rate constants may reflect some partitioning of the quencher between vesicle and aqueous phases. The rapid exit of radical cation from the vesicle is consistent with the measured rate constant of $\sim 2 \times 10^6$ s^{-1} for exit of the TMP radical cation from neutral Triton X-100 micelles (16).

The rapidly decaying component for TMP may be a short-lived radical cation solubilized in a site that leads to rapid electron recombination rather than exit from the vesicle interface region. This is consistent with the fact that fluorescence spectra show clear evidence for at least two different localization sites for TMP in vesicles. We reasoned that photoionization of 7-EHC should give a radical cation that would be much less likely to exit the vesicle, since it would be anchored by the long hydrocarbon chain. This would also reduce the possibility of excitation/photoionization of probe in the aqueous phase.

Since 7-EHC had not been studied in our earlier work on photoionization of coumarins, we used chloranil photosensitization in acetonitrile to generate an authentic spectrum of 7-EHC radical cation (Fig. 6). The spectrum is similar to those obtained previously for other coumarins, although interestingly the long wavelength absorption band is the most red-shifted that we have observed at 700 nm. Excitation of 7-EHC in oxygen-saturated DMPC vesicles resulted in the formation of a short-lived signal ($k_d \sim 7 \times 10^6$ s^{-1}) between 600 and 720 nm that is assigned to a mixture of 7-EHC radical cation and solvated electron. A triplet signal at ~500 nm that decays with a rate constant of $\sim 5 \times 10^5$ s^{-1} is also observed for nitrogen-purged samples. Interestingly, the decay kinetics at long wavelength are similar for nitrogen, oxygen and N_2O degassed samples. The observation of a relatively short-lived radical cation from both TMP and 7-EHC is consistent with decay within the vesicle for the more hydrophobic substrates for which exit of both probe and radical cation is less likely.

CONCLUSIONS

Both steady-state and time-resolved fluorescence spectroscopy demonstrate that psoralens and coumarins are bound to multiple sites in HSA complexes, on the basis of the complex decay kinetics and also in some cases on the relatively broad fluorescence spectra observed. The binding sites show a range of polarities intermediate between those for water and acetonitrile. Interestingly the results for 7-HOC provide the most unequivocal evidence for two binding sites, only one of which is sufficiently aqueous to allow for excited-state deprotonation. Transient spectroscopy results indicate that the radical cation of 6,7-DMC can be generated by photoionization in the HSA complex, but only at specific coumarin/protein ratios. This suggests that the distribution of coumarins among binding sites modifies either the photoionization yield or the lifetime of the initial radical cation. Although we have not been able to provide unequivocal evidence for radical cation formation for other substrates, we cannot rule out the possibility that radical cations are formed but are rapidly trapped by adjacent amino acids in some of the binding sites.

Psoralens and coumarins in vesicles are photoionized with similar efficiencies to micelles and aqueous solution. Our data are consistent with rapid exit ($>2 \times 10^6$ s^{-1}) of the radical cation to the aqueous phase for methoxycoumarins and TMP. By contrast, we observe a population of shorter-lived radical cation that is hypothesized to decay by electron recombination for both TMP and 7-EHC. Such radical cations would be expected to decay by reaction with unsaturated lipids in natural membranes, thereby contributing to membrane damage. These results indicate that electron transfer processes initiated by photoionization of psoralens and coumarins should be considered as a possibility for explaining the chemistry of these substrates both in membranes and as complexes with proteins.

REFERENCES

1. Gasparro, F. P. (1988) *Psoralen DNA Photobiology*, Vols. I and II. CRC Press, Boca Raton.
2. Gonzalez, E. (1995) PUVA for psoriasis. *Dermatol. Clin.* **13**, 851–866.
3. Pathak, M. A. and T. B. Fitzpatrick (1992) The evolution of photochemotherapy with psoralens and UVA (PUVA): 200 BC to 1992 AD. *J. Photochem. Photobiol. B: Biol.* **14**, 3–22.
4. Goodrich, R. P. and M. S. Platz (1997) The design and development of selective, photoactivated drugs for sterilization of blood products. *Drugs Future* **22**, 159–171.
5. Stern, R. S., K. T. Nichols and L. H. Vakeva (1997) Malignant melanoma in patients treated for psoriasis with methoxsalen (psoralen) and Ultraviolet A radiation (PUVA). *New Engl. J. Med.* **336**, 1041–1045.
6. Young, A. R. (1990) Photocarcinogenicity of psoralens used in PUVA treatment: present status in mouse and man. *J. Photochem. Photobiol. B: Biol.* **6**, 237–247.
7. Blan, Q. A. and L. I. Grossweiner (1987) Singlet oxygen generation by furocoumarins: effect of DNA and liposomes. *Photochem. Photobiol.* **45**, 177–183.
8. Bordin, F., M. T. Conconi and A. Capozzi (1987) Certain singlet oxygen quenchers affect the photoreaction between 8-MOP and DNA. *Photochem. Photobiol.* **46**, 301–304.
9. Giles, A. J., W. Wamer and A. Kornhauser (1985) *In vivo* protective effect of ß-carotene against psoralen phototoxicity. *Photochem. Photobiol.* **41**, 661–666.
10. Sastry, S. S. (1997) Isolation and partial characterization of a novel psoralen–tyrosine photoconjugate from a photoreaction of psoralen with a natural protein. *Photochem. Photobiol.* **65**, 937–944.

11. Sastry, S. S., B. M. Ross and P. P'arraga (1997) Cross-linking of DNA-binding proteins to DNA with psoralen and psoralen furan-side monoadducts. *J. Biol. Chem.* **272**, 3715–3723.
12. Schmitt, I. M., S. Chimenti and F. P. Gasparro (1995) Psoralen–protein photochemistry—a forgotten field. *J. Photochem. Photobiol. B: Biol.* **27**, 101–107.
13. Dall'Acqua, F. and P. Martelli (1991) Photosensitizing action of furocoumarins on membrane components and consequent intracellular events. *J. Photochem. Photobiol. B: Biol.* **8**, 235–254.
14. Caffieri, S., A. Daga, D. Vedaldi and F. Dall'Acqua (1988) Photoaddition of angelicin to linoleic acid methyl ester. *J. Photochem. Photobiol. B: Biol.* **2**, 515–521.
15. Waszkowska, E., Z. Zarebska, J. Poznanski and I. Zhukov (2000) Spectroscopic detection of photoproducts in lecithin model system after 8-methoxypsoralen plus UV-A treatment. *J. Photochem. Photobiol. B: Biol.* **55**, 145–154.
16. Chen, L., P. D. Wood, A. Mnyusiwalla, J. Marlinga and L. J. Johnston (2001) Electron transfer reactions in micelles; dynamics of psoralen and coumarin radical cations. *J. Phys. Chem. B.* **105**, 10927–10935.
17. Wood, P. D. and L. J. Johnston (1997) Generation and characterization of psoralen radical cations. *Photochem. Photobiol.* **66**, 642–648.
18. Wood, P. D. and L. J. Johnston (1998) Photoionization and photosensitized electron transfer reactions of psoralens and coumarins. *J. Phys. Chem.* **102**, 5585–5591.
19. Wood, P. D., A. Mnyusiwalla, L. Chen and L. J. Johnston (2000) Reactions of psoralen radical cations with biological substrates. *Photochem. Photobiol.* **72**, 155–162.
20. Peters, T. (1985) Serum albumin. *Adv. Protein Chem.* **37**, 161–245.
21. Dardare, N. and M. S. Platz (2002) Binding affinities of commonly employed sensitizers of viral inactivation. *Photochem. Photobiol.* **75**, 561–564.
22. Berg, K. and J. Moan (1997) Lysosomes and microtubules as targets for photochemotherapy of cancer. *Photochem. Photobiol.* **65**, 383–388.
23. Geibler, D., W. Kresse, B. Wiesner, J. Bendig, H. Kettenmann and V. Hagen (2003) DMACM-caged adenosine nucleotides: ultrafast phototriggers for ATP, ADP, and AMP activated by long-wavelength irradiation. *ChemBioChem.* **4**, 162–170.
24. Curtin, B., P. H. M. Kullmann, M. E. Bier, K. Kandler and B. F. Schmidt (2005) Synthesis, photophysical, photochemical and biological properties of caged GABA, 4-[[2H-1-benzopyran-2-one-7-amino-4-methoxy)carbonyl]amino] butanoic acid. *Photochem. Photobiol.* **81**, 641–648.
25. Bohne, C., R. W. Redmond and J. C. Scaiano (1991) Photophysical techniques. In *Photochemistry in Organized and Constrained Media* (Edited by V. Ramamurthy), Ch. 3. VCH Publishers, New York.
26. Kazanis, S., A. Azarani and L. J. Johnston (1991) Diffuse reflectance laser flash photolysis studies of reactions of triplet benzophenone with hydrogen donors on silica. *J. Phys. Chem.* **95**, 4430–4435.
27. Muthuramu, K. and V. Ramamurthy (1984) 7-Alkoxycoumarins as fluorescence probes for microenvironments. *J. Photochem.* **26**, 57–64.
28. Paik, Y. H. and S. C. Shim (1991) Photophysical properties of psoralens in micellar solutions. *J. Photochem. Photobiol. A: Chem.* **56**, 349–358.
29. Fromherz, P. (1989) Lipid coumarin dye as a probe of interfacial electrical potential in biomembranes. *Methods Enzymol.* **171**, 376–387.
30. Fernandez, M. S. and P. Fromherz (1977) Lipoid pH indicators as probes of electrical potential and polarity in micelles. *J. Phys. Chem.* **81**, 1755–1761.
31. Kraayenhof, R., G. J. Sterk and H. W. Sang (1993) Probing membrane interfacial potential and pH profiles with a new type of float-like fluorophore positioned at varying distance from the membrane surface. *Biochem.* **32**, 10057–10066.
32. Pal, R., W. A. Petri, V. Ben-Yashar, R. W. Wagner and Y. Barenholz (1985) Characterization of the fluorophore 4-heptadecyl-7-hydroxycoumarin: a probe for the head-group region of lipid bilayers and biological membranes. *Biochem.* **24**, 573–581.
33. Zaton, A. M. L. and J. P. Villamor (2001) Study of heterocycle rings binding to human serum albumin. *Chem. Biol. Interactions.* **124**, 1–11.
34. Vorum, H., K. Fisker and R. Brodersen (1994) High-affinity binding of two molecules of warfarin and phenprocoumon to human serum albumin. *Biochim. Biophys. Acta.* **1205**, 178–182.
35. He, X. M. and D. C. Carter (1992) Atomic structure and chemistry of human serum albumin. *Nature* **358**, 209–215.
36. Dockal, M., D. C. Carter and F. Rxuker (1999) The three recombinant domains of human serum albumin. *J. Biol. Chem.* **274**, 29303–29310.
37. Dahlquist, F. W. (1978) The meaning of Scatchard and Hill plots. *Methods Enzymol.* **48**, 799–804.
38. McGimpsey, W. G. and H. Gorner (1996) Photoionization of indole, N-methylindole and tryptophan in aqueous solution upon excitation at 193 nm. *Photochem. Photobiol.* **64**, 501–509.